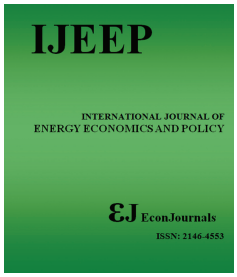

International Journal of Energy Economics and Policy

ISSN: 2146-4553

available at http: www.econjournals.com

International Journal of Energy Economics and Policy, 2019, 9(3), 280-290.

Performance Optimization of Constant Speed - Small Horizontal Axis Wind Turbine for Wind Energy Development in Malaysia

Tan Woan Wen, C. Palanichamy*, Gobbi Ramasamy

Faculty of Engineering, Multimedia University, 63100 Cyberjaya, Selangor DE, Malaysia. *Email: drcpc1119@gmail.com

Received: 14 January 2018 **Accepted:** 20 March/2019 **DOI:** https://doi.org/10.32479/ijeep.7567

ABSTRACT

Though Malaysia is blessed with a lot of natural resources, still it mainly depends on fossil-fuels for electricity generation. Due to this dependency, among the different polluting agencies, the electric power sector ranks second in the country's statistics. So as to reduce the pollution from them and to reduce the dependency on the depleting fossil-fuels, Malaysia is very keen on promoting renewable energy based electricity generation. Following the Government's renewable energy policy and subsidies, several renewable energy attempts were made and only the solar PV energy systems have had a good start; however, the continued development from the start is questionable because of the high capital cost involved and the unattractive energy conversion efficiency. Few attempts on the proven, cost-effective wind energy systems were carried out and the net outcome is not encouraging due to the low-speed scenario in Malaysia. As per a few successful studies on wind speed assessments, there are attractive sites for wind turbine based electricity generation not with high speed higher capacity turbines, but at low speed small capacity wind turbines. To promote wind energy in Malaysia and to attract global investors, this research aims at low capacity wind turbines suitable for low wind regimes as in the Malaysian context. The proposed constant speed-small horizontal axis wind turbines exhibited encouraging values of annual energy production, power coefficient and capacity factors promising a successful start of wind energy in Malaysia.

Keywords: Low End Speed Regimes, Small Wind Turbines, Energy Sustainability, Blade Element Momentum Theory
JEL Classifications: Q42, Q48, Q55, Q56

1. INTRODUCTION

Wind energy is an encouraging and cost-effective source of renewable energy and is successfully practiced in several parts of the world (Azad and Saha, 2012). Though there are different sizes of wind turbines available in the market, only the larger wind turbines (IRENA, 2017; The European Offshore Wind Industry, 2018) have become more industrious due its attractive cost of energy production and rapid payback period. Still, a major portion of the world could not implement them in large scale because of insufficient wind potential in their region to generate the designated power. Also, large wind turbines are capital intensive and require a large extent of land. Nowadays, the distributed generation (DG) concept (Duləu et al., 2014; Munish, 2018) is gaining interest among energy producers and domestic consumers aiming at off-grid and remote location electrification facilities. For such applications, small wind turbines (SWTs) (Manoj and Roy, 2015) become the right choice as an alternative source of electricity.

Developing countries in the South-East Asian region like Malaysia, Brunei, and Indonesia are in the process of promoting renewable sources as the means of utilizing their freely available wind and solar power to overcome their environmental issues and to preserve their fossil-fuel reserves. In Malaysia, as a tropical country, the solar energy is abundant, but the wind potential is very weak (MMD, 2016). Demonstration projects in wind energy resulted in failure, which is a practical evidence for the scarce

wind speed in Malaysia. Though solar energy is plentiful, it is capital intensive and less efficient (only 14% as the maximum efficiency) compared to other sources of renewable energy. As per the available wind statistics, Malaysia is for the most part known to encounter low wind speeds, and consequently larger wind turbine is certainly not an attainable sustainable power source (Palanichamy et al., 2015). In any case, there are a few territories in Malaysia experience strong wind during certain periods in a year. Moreover, the earlier wind statistics indicate that the mean annual wind speed is in the range of 2-3 m/s which is suitable for small wind turbines not exceeding 100 kW capacity, which is ideal for distributed generation implementation (Tan and Palanichamy, 2018). Hence, this proposed research focuses on the aerodynamic optimization design for constant speed-small horizontal axis wind turbine (CS-SHAWT). This is by considering the prevailing wind condition in Malaysia and experimenting with six different low-Reynolds number aerodynamic characteristic airfoils. The experimental results exhibit the annual energy yield, power coefficient and capacity factors of the six CS-SHAWTs. The performance analysis is done by the mathematical model of the blade element momentum theory.

2. MALAYSIAN WIND POTENTIAL

For successful wind energy harnessing in any region, the imperative factor of executing wind turbine is the readiness of durable wind. Malaysia with tropical nature is in general identified to encounter low wind speeds, and in this way wind energy conversion technology is definitely not a practical sustainable source of energy at the larger level. Though the wind is capricious and gentle, there are a few territories in Malaysia have durable wind speed in the range of 5-15 m/s during certain periods in a year (Palanichamy, 2015). As per the Malaysia Meteorological Department (MMD), there are three monsoons based on the wind flow patterns as depicted in Figure 1.

From the meteorological information seen in Figure 1, the favourable period for wind turbine performance is the North East monsoon during November to March (Five months). The wind flow duration for about 5 months is as attractive as that of the proven windy sites in Tamil Nadu, Maharashtra, Gujarat, Rajasthan and Karnataka states in India and Nebraska, Kansas, South Dakota, North Dakota, and Iowa states in USA and the only difference is the mean annual wind speed which is not as great as in Indian and American sites.

An assessment based on the meteorological data from 2006 to 2015 for two stations shown in Figure 2a and b confirms the fertile period for wind energy harvesting as November to March.

The basic wind speeds are customarily measured at 10 m height above ground level at all meteorological stations. The statistical approach performed in 2009 (Yong et al., 2011) identified the best windy sites of Malaysia with a mean annual wind speed above 2 m/s as depicted in Table 1. According to the Malaysia Meteorological Department (MMD, 2016), the highest mean daily wind speed at 10 m height above ground level is 3.8 m/s, logged at Mersing, Johor state, while the highest maximum wind speed is 41.7 m/s, recorded in Kuching, Sarawak state on 15th September 1992. Average Weibull shape parameter and scale parameter were found to be 1.76 and 3.21 m/s, respectively. Yearly mean wind speed in Kuala Terengganu is 2.9 m/s and the monsoon season (November to March) mean wind speed is 3.9 m/s.

Though all the sites listed in Table 1 have a mean annual wind speed of 2 m/s and above at 10 m height, their frequency distribution varies considerably as shown in Table 2. The Mersing site has a wind availability period of 67.35% per annum at a power generating wind speed of 2 m/s, and the other sites as Kudat (50.91%), Sandakan (57.08%), Pulau Langkawi(40.81%), and Kuala Terengganu (36.87%). These figures are encouraging as compared to the proven global wind sites in India and US; but the cut-in wind speed which is less suitable for small wind turbine of low cut-in wind speeds.

Figure 1: Mansions based on wind flow patterns

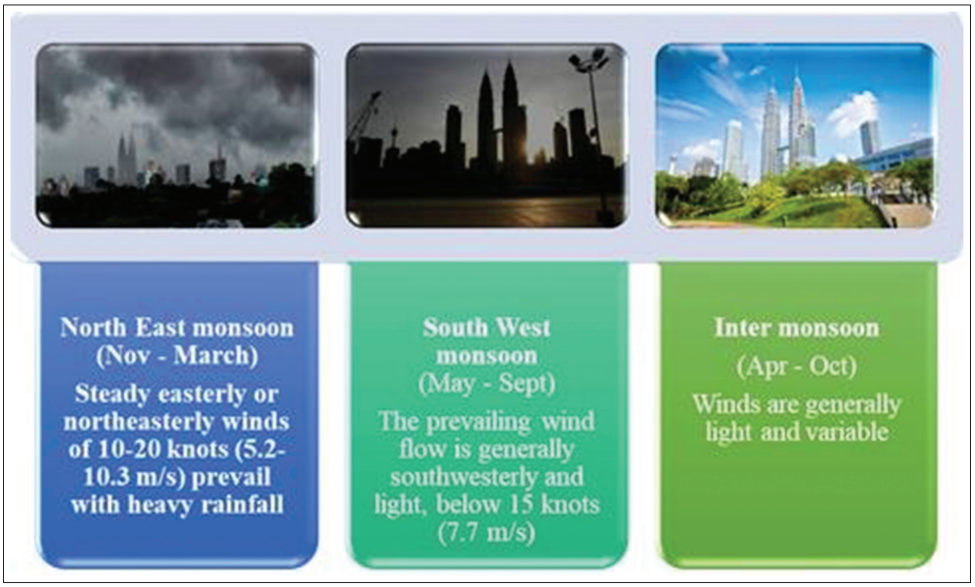

3. SUITABILITY OF COMMERCIAL WIND TURBINES IN MALAYSIA

Eight commercially available SWTs in the range of 0.4 kW to 5.8 kW were considered for the research. Table 3 shows the study outcome of the SWTs with different rotor swept areas considering five locations in East Malaysian, portraying the predicted power coefficient and the annual energy generation (AEG). According to Betz Law, the maximum of power coefficient (efficiency of energy conversion) is 59% for an ideal scenario. However, this scenario barely happens in the real world due to several factors, which mainly involves losses in the gearbox, generator, and especially the aerodynamic efficiency of the rotor blades, as the wind requires to pass through the rotor blades first so as to start the turbine to generate energy.

Figure 2: (a) Monthly average wind speed in Miri. (b) Average wind speed in Kuching

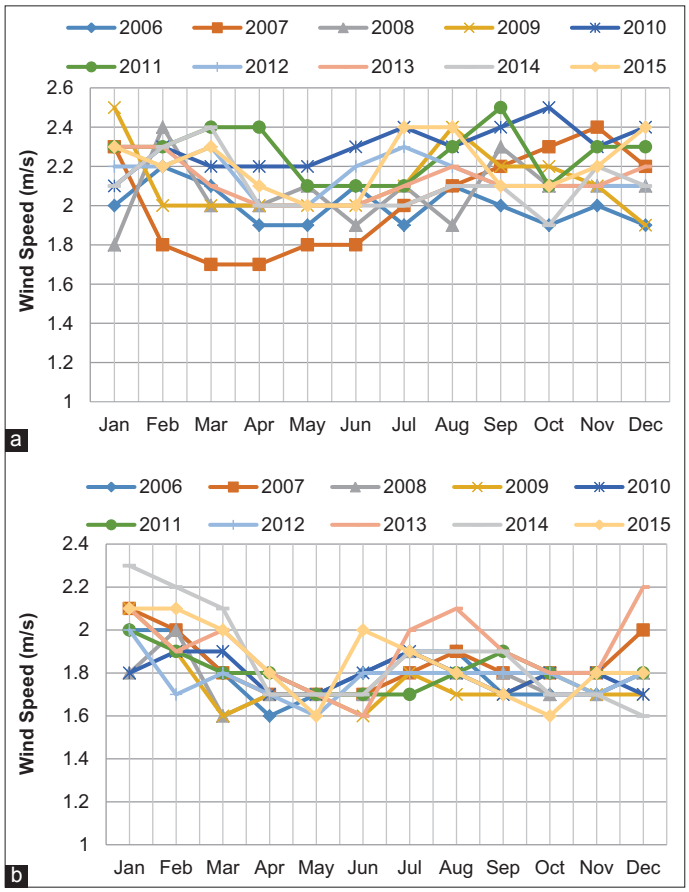

Table 1: Probable wind sites of Malaysia

Site	Mean annual wind speed (m/s) at 10 m anemometer height
Pemanggil Island	4.21
Mersing	3.58
Kudat	2.62
Sandakan	2.49
Pulau Langkawi	2.27
Kota Bahru	2.21
Pulau Terengganu	2.11

As shown in Table 3, the highlighted cells indicate the predicted power coefficient based on the power curve provided by manufacturers has exceeded the Betz limit. Many small wind turbine manufacturers usually provide untruth specification of their turbines to appear superior than their competitors (Samuel et al., 2013). In fact, it is impossible to capture the wind fully especially at earlier wind speeds as most of the small wind turbines rely on the aerodynamic forces to operate. Gipe (2004) and Fasel and Gross (2011) quote that the majority of the commercial small wind turbines' power coefficient is <40% and hardly produce greater than 25% or 30% useful energy when compared to large turbines which have power coefficient values of 45%.

These five locations in East Malaysia lies in 1-2 m/s average wind speed, which is below or near the cut-in speed of the turbine. The cut-in speed of the turbine is the minimum wind speed of the rotor to start rotating. Typically, the commercial small wind turbines are mounted at a relatively lower height, meaning their hub height wind speeds may be very close to their cut-in speed. Though the rotor may turn slowly at these low wind speeds, but the turbine generator would not be generating much of useful energy. The turbine may halt after a certain period.

The major issue in small wind turbines is the laminar separation bubbles occurs on the rotor blades causing it difficult to start at low wind speeds which is due to the low Reynolds number of small-size rotor blade and low wind speeds. The laminar separation bubble is affiliated with low Reynolds where the laminar flow separates before the air transfers to turbulent flow, as a result the overall performance of turbine system degradations in terms of cut-in speed and power coefficients (Ronit et al., 2013; Ozgener and Ozgener, 2011). The starting also depends on the aerodynamic torque and resistive torque, especially for the rotor blade radius <1.5 m; as the rotor begins to rotate only when the aerodynamic torque exceeds the overall resistive torque comprised drive train of the turbine system and generator (Clausen and Wood, 1999). Hence, rotates considerably slowly allows wind to pass through the openings between the blades.

For the reasons stated, the corresponding predicted AEG values presented in Table 4 could not be accurate as well. That is also

Table 2: Probable wind sites based on frequency of average wind speed

Site	Frequency of average wind speed (h)					
	0-1 m/s	1-2 m/s	2-3 m/s	3-4 m/s	4-5 m/s	5-6 m/s
Mersing	400	2200	3050	1450	900	500
Kudat	1800	2270	1790	1320	950	400
Sandakan	1200	3050	2700	1400	700	200
Pulau Langkawi	2200	2900	1900	1150	400	125
Kuala Terengganu	1800	3800	1900	920	290	120

the reason why we should not trust merely based on the AEG results. For example, turbine Fortis Montana of 5.8 kW rated power produces 33.3% of power coefficient at 5 m/s and mapped their power onto the wind speed probability of a location which based on Weibull distribution function, one may still able to get a high value of AEG with a very small wind probability. The failed projects in Malaysia are a good real-world example, because of these reasons. People tend to be blinded by the AEG without doing a proper analysis before making installation. This is not only because of the technical issues and aerodynamic performance of the turbines, and the most crucial factor is the low average wind speed corresponding to the cut-in speed of the turbine.

Other than that, Table 4 also has given us a very essential information when comparing AEG, kWh and the AEG per rotor swept area (kWh/m^2) for all the turbines with different rotor diameter. The AEG per rotor swept area of smaller diameter has the potential of achieving higher performance compared to AEG with larger diameter rotors. This gives us an indication that it is cost-effective when we go for a wind power plant installation of small rotor blade diameter.

Most of the commercially available wind turbines are mainly designed to operate at optimum wind conditions or at higher wind speeds. Therefore, the majority of the commercially available wind turbines are not appropriate for low wind speed sites. Aerodynamic optimization is very significant in designing CS-SHAWT to generate maximum energy from low wind. The optimized small rotor blade size could even compete with the larger rotor blade diameter in the aspects of producing power from capturing maximum wind speeds of the specific locations. By doing so, optimization of flapwise (chord) and settling angle (twist) distribution along the blade span of the rotor blade is one of the factors concerns which will be discussed in the following sections.

4. DESIGN SPECIFICATION

4.1. Initial Design

The CS-SHAWT is a 3-bladed rotor with 1.1 m diameter (rotor radius, R = 0.55 m), hub radius of 0.05 m and blade length of 0.5 m. Based on the international standard of IEC61400-2 for designing small wind turbines, the design wind speed, V_{design} is 3.5 m/s for the mean annual wind speed (MAWS) of 2-3 m/s in Malaysia. The design wind speed is also the value of rated wind speed for CS-SHAWT.

The design tip speed ratio (TSR) of 5 and 6 is chosen for the design wind speed of 3.5 m/s. The chosen value of TSR determines the optimal value of rotational speed which gives 304 rpm and 356 rpm, respectively as listed in Table 5. The TSR value will directly affect the blade rotational speed, ω (in rad/s) and Reynolds number. Hence, the overall turbine performance is affected as well. The special of CS-SHAWT is, it always spins at the constant speed regardless of the wind speed flow through as the TSR would vary with wind speed. CS-SHAWT only reaches its optimum power coefficient at the given wind speed (rated wind speed). A constant pitch of zero angle is applied in CS-SHAWT to eliminate starting issue as well as to expose high flow angle.

$$\text{TSR}: \lambda_{design} = \frac{\omega R}{V_{design}} \quad (1)$$

Table 3: Power coefficient as a function of wind speed of commercial small wind turbines

Turbine	NE1000	NE600	NE400	e160i	e230i	e300i	TES 5kW	Fortis Montana
Rated power (kW)	1	0.6	0.4	0.6	0.8	1	5	5.8
Wind speed (m/s)	Power coefficient, C_p (%)							
1	>59.0	>59.0	>59.0	0	0	0	0	0
2	>59.0	>59.0	>59.0	>59.0	>59.0	28.9	0	0
3	>59.0	>59.0	>59.0	>59.0	54.6	21.4	48.8	30.8
4	>59.0	>59.0	>59.0	38.1	30.7	36.1	50.8	29.2
5	>59.0	>59.0	>59.0	40.6	27.5	27.7	51.9	33.3
6	46.5	>59.0	51.0	37.6	25.0	25.4	49.2	27.9
7	36.4	44.1	43.9	38.5	22.9	23.6	47.3	26.1
8	28.5	36.7	38.8	39.6	23.0	22.6	31.7	23.9
9	24.4	31.4	32.9	37.6	21.6	20.9	22.3	22.8
10	20.8	28.9	27.7	35.5	20.6	20.8	16.2	22.5

Table 4: Predicted AEG and rotor swept area of commercial small wind turbines

Turbine		NE1000	NE600	NE400	e160i	e230i	e300i	TES 5kW	Fortis montana
Rotor diameter (m)		2.8	1.8	1.6	1.6	2.3	3.0	8	5
Miri	kWh	1314	565	341	250	227	109	948	237
	kWh/m^2	213	222	170	124	55	15	19	12
Kuching	kWh	1160	497	303	183	153	8	187	0
	kWh/m^2	188	195	151	100	37	1	4	0
Bintulu	kWh	1117	480	293	146	123	1	144	0
	kWh/m^2	181	189	146	73	30	0	3	0
Sibu	kWh	1040	457	269	109	83	0	65	0
	kWh/m^2	169	180	134	54	20	0	1	0
Sri Aman	kWh	711	321	176	30	2	2	0	0
	kWh/m^2	115	126	88	15	0	0	0	0

AEG: Annual energy generation

In this study, we applied blade element momentum theory (BEMT), which is also known as strip theory to design six CS-SHAWTs with different airfoils. The main advantage of CS-SHAWT is direct connection of grid using induction generator without complex power electronics devices required. This makes CS-SHAWT simple, ease of control, sturdy as well as cost-effective.

4.2. Blade Element Momentum Theory (BEMT)

The classical BEMT is adopted to evaluate the performance of the blade aerodynamic design. The aerodynamic performance is straight away linked to the shape of the blade comprising of airfoils, chord and twist distribution. Blade element momentum (Burton et al., 2001) is a theory that combines both blade element theory and momentum theory which relates to rotor performance with blade geometry, respectively. From the blade element theory, it is assumed that no aerodynamic interactions between different blade elements take place (Manwell and Jon, 2009). Amongst the available methods, BEMT is the most common mathematical model for evaluating wind turbine performance. This classical BEMT is readily practicable, efficient and fast with an economic value in analysing wind turbine aerodynamics. Figure 3 depicts the relationship of velocities and forces acting on the blade element.

In BEMT method of analysis to obtain the maximum power at a particular wind speed, the blade is divided into 10 segments (elements) along its span and two- dimensional experimental lift and drag coefficients are used to determine the aerodynamic forces on each segment. Each segment is examined individually. From the momentum theory, the thrust, dT and torque, dQ for each of the elements are characterized by:

$$dT = \rho V_\infty^2 4a(1-a)\pi r dr \quad (2)$$

Table 5: Chosen TSR with its respective Reynolds number and rotational speed

Parameters	TSR=5	TSR=6
Reynolds number, Re	250,000	300,000
Rotational speed in RPM	304	356

TSR: Tip speed ratio

Figure 3: Blade element velocities and forces

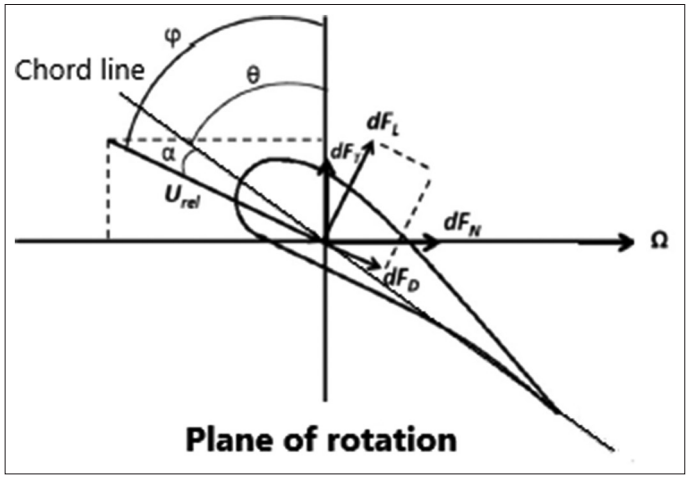

$$dQ = 4a'(1-a)\rho V_\infty \pi r^3 \Omega dr \quad (3)$$

Where r is the radial location along the blade length, Ω is angular velocity, a and a' are axial and angular induction factors, respectively.

It is assumed that no aerodynamic interactions between different blade elements take place (Manwell and Jon, 2009); the normal force, F_n and torque, Q is determined as follows:

$$dF_n = B\frac{1}{2}\rho U_{rel}^2 (C_l \cos\varphi + C_d \sin\varphi) c dr \quad (4)$$

$$dQ = B\frac{1}{2}U_{rel}^2 (C_l \sin\varphi + C_d \cos\varphi) c dr \quad (5)$$

Where B is the number of blades, ρ is air density, U_{rel} is the relative wind speed, C_l and C_d are lift and drag coefficients depend on Reynolds number and the angle of attack, respectively, and φ is the relative angle.

After paralleling normal force and torques from blade element and momentum theory, the valuable correlation for axial and angular induction factors has resulted. They are used to govern the angle of relative wind and angle of attack which results in reading lift and drag coefficient. Additionally, tip loss factor is incorporated in BEMT according Prandtl theory (Manwell and Jon, 2009) as given in Equation (6). Subsequently, a and a' are rationalized for each blade element as given in Equations (7) and (8).

$$F = \left(\frac{2}{\pi}\right)\cos^{-1}\left[\exp\left(-\left(\frac{\left(\frac{B}{2}\right)\left[1-\left(\frac{r}{R}\right)\right]}{\left(\frac{r}{R}\right)\sin\varphi}\right)\right)\right] \quad (6)$$

$$a = \frac{1}{1+\frac{4F\sin^2\varphi_i}{\sigma' C_l \cos\varphi_i}} \quad (7)$$

$$a' = \frac{1-3a}{4a-1} \quad (8)$$

The process is repetitive till axial and angular induction factors are converged. The power coefficient, C_p is calculated as given in Equation (9), after the rotor torque and power are obtained.

$$C_P = \frac{P}{\frac{1}{2}\rho\pi R^2 V^3} \quad (9)$$

4.3. Airfoils

Six airfoils are selected for designing CS-SHAWT which are BW-3, FX63-137, NACA4412, S822, SG6040 and SG6043. They are tailored for use on small horizontal axis wind turbine applications which operate at low Reynolds (Re) number below Re = 500,000 (Giguere and Selig, 1997) i.e., to operate at low wind speed. Choosing suitable airfoil is significant because the performance of the rotor blade depends on aerodynamic design; their cross-section is as shown in Figure 4.

Figure 4: Cross-section of selected airfoils

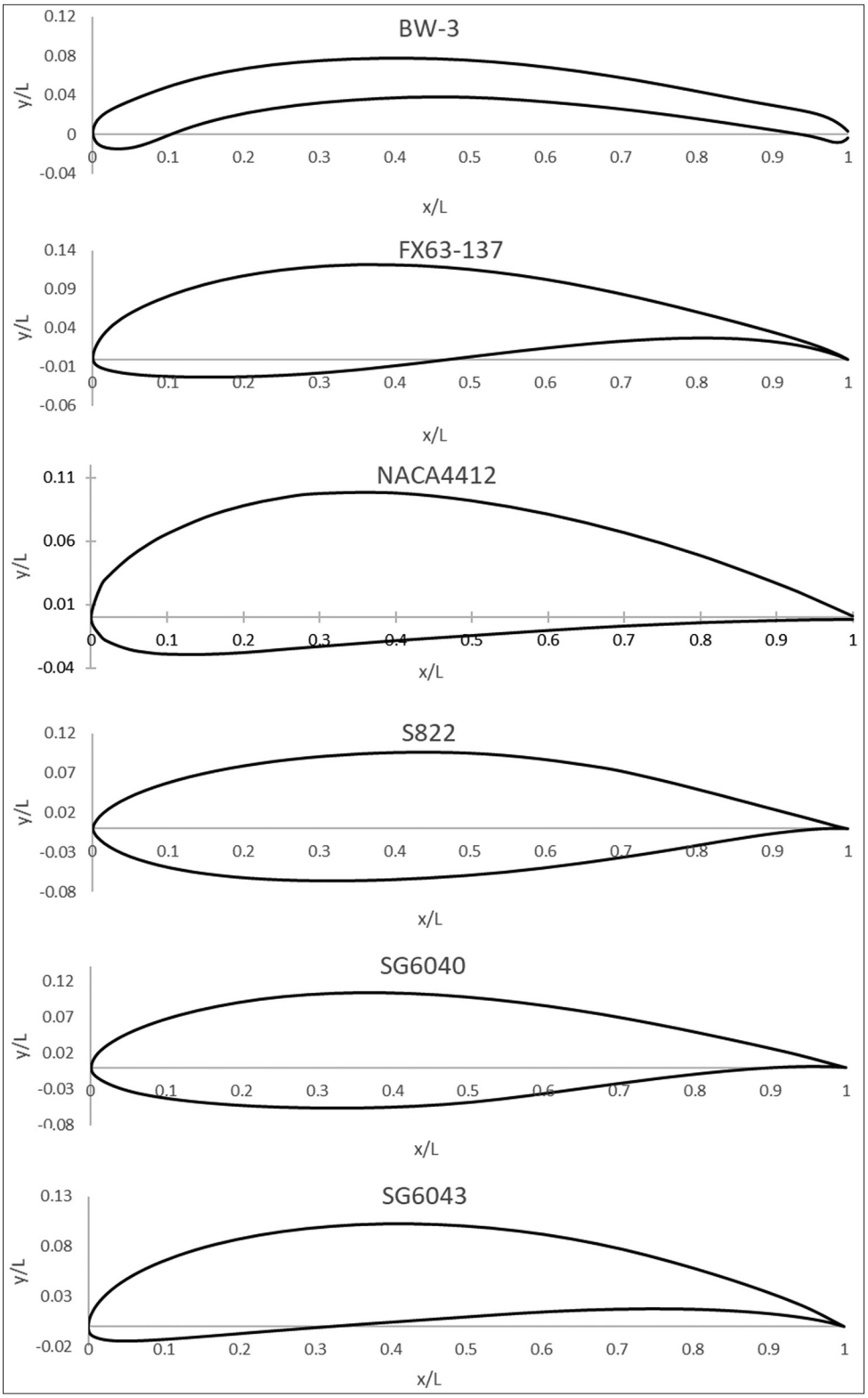

4.3.1. BW-3 airfoil

BW-3 airfoil is designed by Bergey, (2018) Windpower company for their wind turbine system which is widely commercialized in the market around the globe. BW-3 has a maximum thickness of 5% of the airfoil chord length, which is considered as relatively low compared to other low Reynolds number airfoils. The key features of the BW-3 airfoil are no formation of large separation bubbles at low Reynolds number in contrast to thicker airfoils. This model permits the turbine to have a lower cut-in speed at desired lift coefficient.

4.3.2. FX63-137 airfoil

The Wortmann FX63-137 airfoil (Wortmann, 2018) is suitable for small wind turbines applications at the trailing edge of airfoil is cusped in the Reynolds range of 100,000 to 500,000 during McGranahan and Selig (2004) testing; this phenomenon indicates aerodynamic loading enhances within the cusped region. One of the attractiveness of the Worthmann FX63-137 airfoil is its high-lift coefficient amongst the low Reynolds number airfoils model.

4.3.3. NACA4412 airfoil

The NACA4412 airfoil is developed by the National Advisory Committee for Aeronautics (NACA). The four digits refer to maximum camber of 4% of chord located at 40% chord back from the leading edge and thickness is 12%. This model is nearly a flat bottom surface avoids the negative ground effect that happens with extreme curvature or when Venturi flow is created beneath the airfoil. According to (Cosker, 2012), NACA4412 has desirable average power coefficient values of a wider range of TSR.

4.3.4. S822 airfoil

The S822 airfoil is developed under a joint between the National Renewable Energy Laboratory (NREL and Airfoils, Inc., 2014). This airfoil has 16% thickness at its sections allows a reduced roughness sensitivity for increased energy capture under overall rough performance of the airfoil; due to its feature, it permits for an increased stiffness and enhanced fatigue resistance makes it favourable to use for CS-SHAWT system.

4.3.5. SG6040 and SG6043 airfoils

The SG6040 and SG6043 airfoils are the series of thin airfoil family designed specifically for the small wind turbine blades operating in the low Reynolds range of 100,000 to 500,000 (Giguere and Selig, 1998). Basically, thin airfoil is designed for operating at low Reynolds applications because this type of model can reduce the suction peak near the leading edge to lessen the adverse pressure gradient in order to avoid laminar flow separation on the surface layer.

Table 6 shows the geometrical characteristics of selected six airfoils and as given in Figure 5 is the illustration of an airfoil. Theoretically, the air flows across the upper and lower surface of airfoil generates lift and drag forces by its differences pressure, which is leading the net force in the perpendicular direction of wind flow as depicted in Figure 3. The aerodynamic forces are the main cause to rotate the rotor blade of a wind turbine. This is the reason of innumerable airfoil shapes available in the market nowadays. Selecting suitable airfoils based on the wind regimes is a crucial task.

The given Reynolds number does not change along the blade because of the constant rotor speed, except the TSR and the angle of attack changes according to wind flows. As shown in Table 7a and b are the airfoil characteristics for TSR of 5 and 6. These parameter values for maximum C_L/C_D and angle of attack are obtained from a foil and they are depending on the Reynolds number. Therefore, the given outcome of six airfoils is in optimal values. This is directly influencing the optimum power coefficient of CS-SHAWTs as all the parameters are interrelated to one another. The small wind turbine has low Reynolds number airfoil (<Re = 500,000) compared to large wind turbine. As following shows the equation of Reynolds number, it is the function of air viscosity μ, relative wind speed V_{rel}, air density ρ as well as the chord length of airfoil, c.

$$\text{Reynolds number, } Re = \frac{\rho V_{rel} c}{\mu} = \frac{\text{Inertia force}}{\text{Viscous force}} \quad (10)$$

The corresponding lift, drag and lift-to-drag coefficient at different angles of attack for Re = 250,000 (TSR of 5) are shown in Figure 6a-c and Re = 300,000 (TSR of 6) are shown in Figure 6d-f. The combination of maximum lift force and minimum drag force form the lift-to-drag ratio. High lift-to-drag ratio contributes to high start-up torque that is leading good response at low wind speed in order to maximise power generation which is highly desirable for small rotor size.

The chord length of each element of the blade can be calculated as given in Equation (11). The final chord length distributions are as shown in Figure 7a and c for TSR of 5 and 6, respectively. To calculate the twist angle of the blade, Equation (12) is applied to calculate the angle of the relative wind, φ_r at each blade section.

Table 6: Maximum thickness and chamber for selected airfoils

Airfoil	Maximum thickness (%), t/L	Maximum camber (%), c/L
BW-3	5.0	5.7
FX63-137	13.7	5.8
NACA4412	12.0	4.0
S822	16.0	1.8
SG6040	16.0	2.3
SG6043	10.0	5.1

Figure 5: Geometry of airfoil

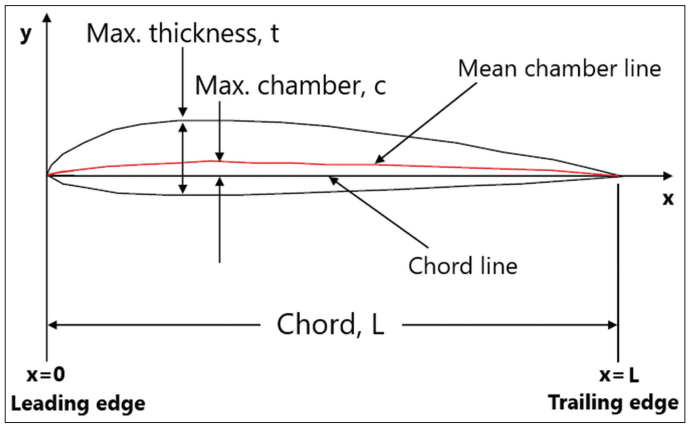

Figure 6: (a) Lift coefficient for Re 250,000 (tip speed ratio [TSR] = 5). (b) Drag coefficient for Re 250,000 (TSR = 5). (c) Lift/drag coefficient for Re 250,000 (TSR = 5). (d) Lift coefficient for Re 300,000 (TSR = 6). (e) Drag coefficient for Re 300,000 (TSR = 6). (f) Lift/drag coefficient for Re 300,000 (TSR = 6)

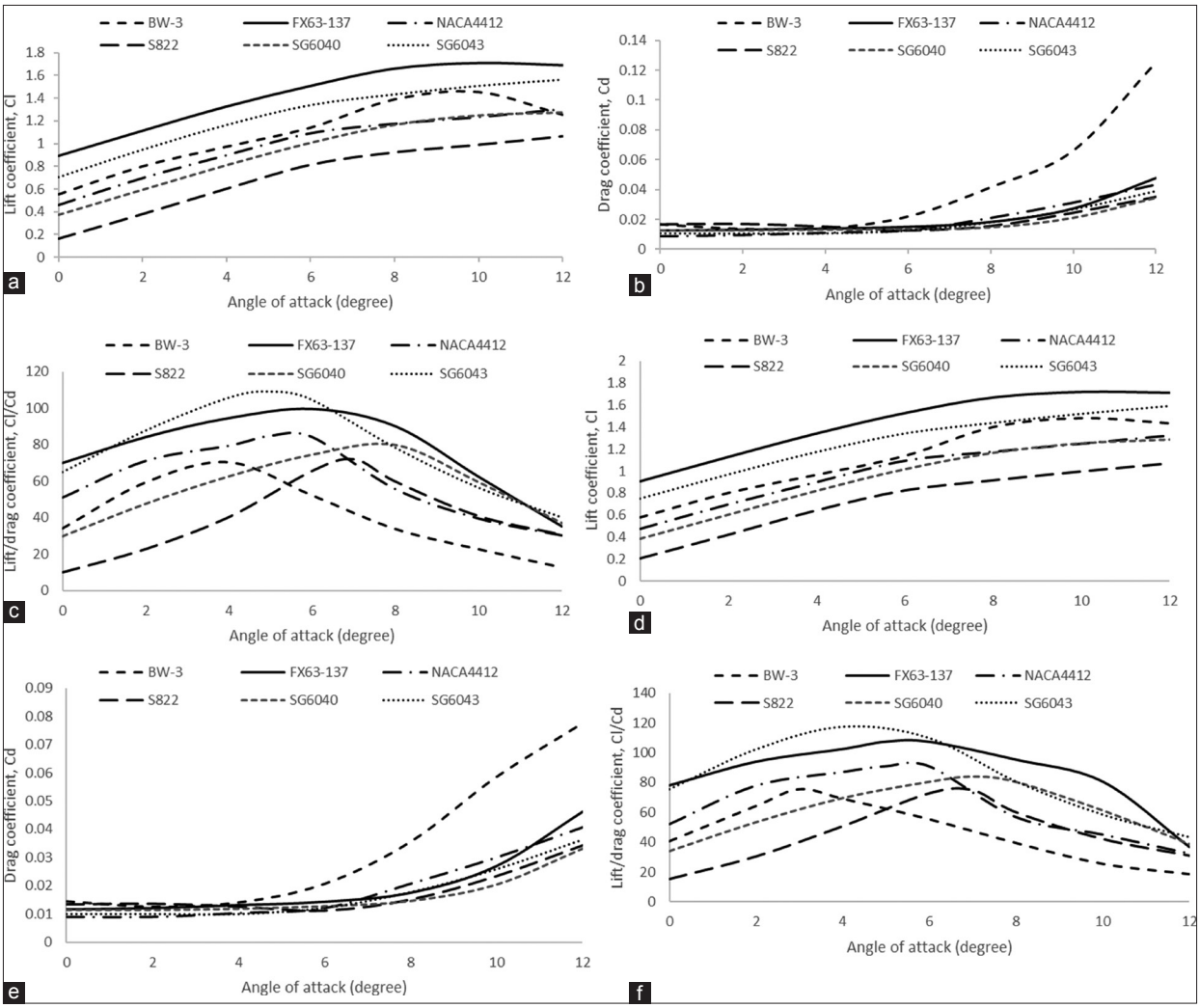

Figure 7: (a) Chord distributions for tip speed ratio (TSR) = 5. (b) Twist distributions for TSR = 5. (c) Chord distributions for TSR = 6. (d) Twist distributions for TSR = 6

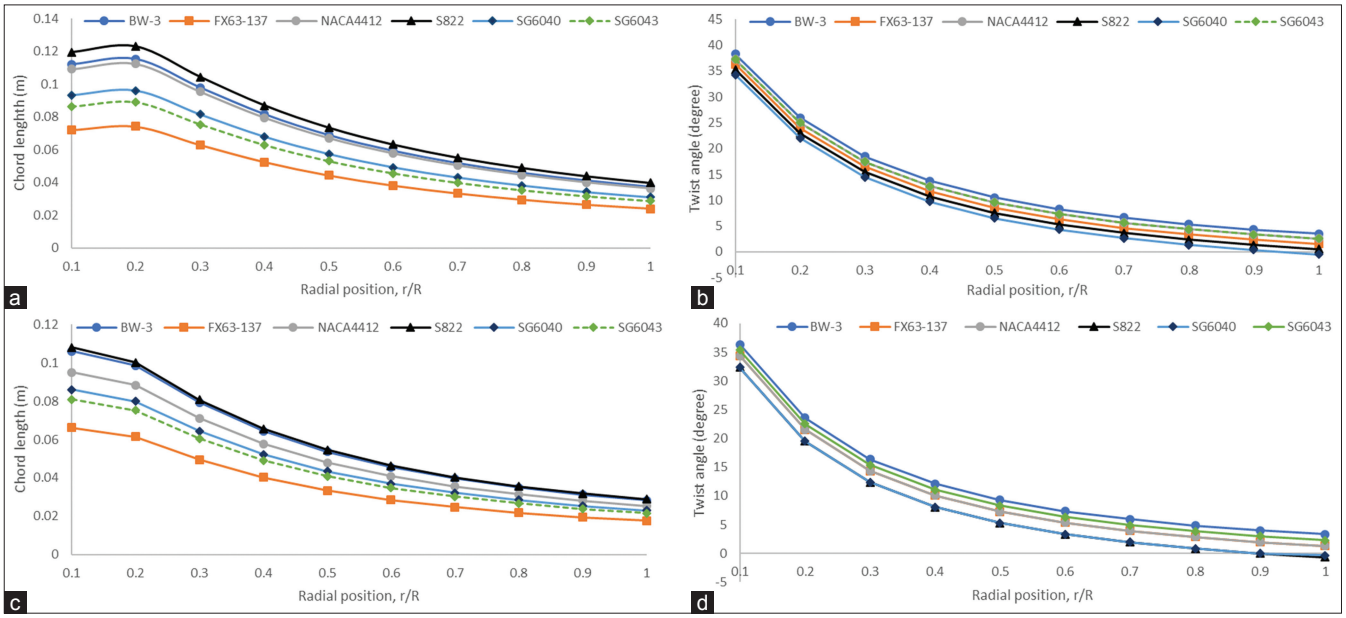

Then, twist angle can be calculated by Equation (13) and the resultant twist angle distribution of the blade for TSR of 5 and 6 are presented in Figure 7b and d, respectively.

$$c_r = \frac{8\pi r_r}{BC_{l,r}}(1-\cos\varphi_r) \quad (11)$$

$$\varphi_r = \tan^{-1}\left(\frac{(1-a)}{(1+a')\lambda_r}\right) \quad (12)$$

$$\beta_r = \varphi_r - \alpha_{airfoil} \quad (13)$$

5. RESULTS AND DISCUSSION

5.1. Annual Energy Generated, AEG

The power generated by a wind turbine mainly depending on both the design characteristics of the turbine and the properties of the wind resource. It is important to choose the site carefully to know the capability of our designed CS-SHAWTs. The wind distribution at Kangar with mean annual wind speed (MAWS) of, v = 2.53 m/s is chosen, because our design wind speed for CS-SHAWTs is 3.5 m/s which is the MAWS of 2.5 m/s in Malaysia (2-3m/s). The popular Weibull distribution function, F(v) is used to compute the wind speed statistic for wind engineering applications, with the given shape factor, k of 2.01 and the scale of wind regimes, C of 2.86 m/s as presented in the following equation (Irwanto et al., 2014), and the probability density function of MAWS at Kangar is shown in Figure 8.

$$F(v)=\left(\frac{k}{C}\right)\left(\frac{v}{C}\right)^{k-1} e^{\left(-\frac{v}{c}\right)^k} \quad (14)$$

The power curve, P(v) of the designed CS-SHAWTs as depicted in Figure 9a and b is mapped with Weibull distribution function, F(v). To compute the annual energy generated (AEG), $E_{generated}$ Equation (15) is used with annual hours, T as 8760 and the results are shown in Table 8. The results show that the SG6043 turbine has the highest AEG in both TSR of 5 and 6, which are 64 kWh and 66 kWh respectively, whilst the lowest AEG turbine for TSR of 5 is BW-3 with only 59 kWh and for TSR of 6 is S822 with 56 kWh. It is obvious that the airfoil plays a vital role in achieving optimum performance. Based on the values given in Table 7a and b, SG6043 airfoil has the highest values in the $(C_L/C_D)_{max}$ ratios in both TSR of 5 and 6. Hence, it is noticeable that the aerodynamic performance of an airfoil can be enhanced by increasing the lift force and reducing the drag force.

$$E_{generated} = T\int P(v)F(v)dv \quad (15)$$

5.2. Power Coefficient

The power coefficients for six turbines are shown in Figure 10a and b. The maximum power coefficient at TSR 5 and 6 are summarised in Table 9. The results illustrate that all turbines have a higher optimum power coefficient at TSR of 5 than TSR of 6, which is due to the rotational speed and the cut-in speed of designed CS-SHAWTs. As given in Table 10 the cut-in speed for all turbines at TSR of 5 is lower compared to TSR of 6. This allows the turbine to start generating electricity at lower wind speed and lower rotational speed. The rotational speed for TSR of 5 is 304 rpm while for TSR of 6 is 365 rpm, which confirms that lower TSR is desirable for low MAWS. In other words, the aerodynamic performance of airfoil increases exponentially as the Reynolds number increases, giving lower cut-in speed as well as the higher power coefficient.

In the aspect of power coefficient; the highest C_p value for TSR of 5 and 6 is SG6043 and FX63-137 turbine with 0.5194 and 0.5148, respectively. Both turbine's cut-in speed is nearly the same, which is 1.78 and 1.76, respectively. However, in the aspect of cut-in speed, the BW-3 and FX63-137 turbine have the similar lowest start-up of 1.50 m/s at TSR of 5, whilst S822 turbine starts at 1.58 m/s. Turbines, which have low cut-in speed are highly favourable for low wind speed as well.

Table 7a: Airfoils' characteristics for Re=250,000 for TSR=5

Airfoil	$(C_L/C_D)_{max}$ ratio	Angle of attack, α	Lift coefficient, C_L
BW-3	70.48	4	0.9736
FX63-137	99.53	6	1.5120
NACA4412	84.82	5	0.9980
S822	71.99	7	0.9132
SG6040	79.77	8	1.1678
SG6043	109.10	5	1.2630

Table 7b: Airfoils' characteristics for Re=300,000 for TSR=6

Airfoil	$(C_L/C_D)_{max}$ ratio	Angle of attack, α	Lift coefficient, C_L
BW-3	75.41	3	0.896
FX63-137	107.17	5	1.4360
NACA4412	91.03	5	1.0000
S822	75.10	7	0.8810
SG6040	83.84	7	1.1050
SG6043	117.25	4	1.1758

TSR: Tip speed ratio

Figure 8: Probability density function of mean annual wind speed at Kangar

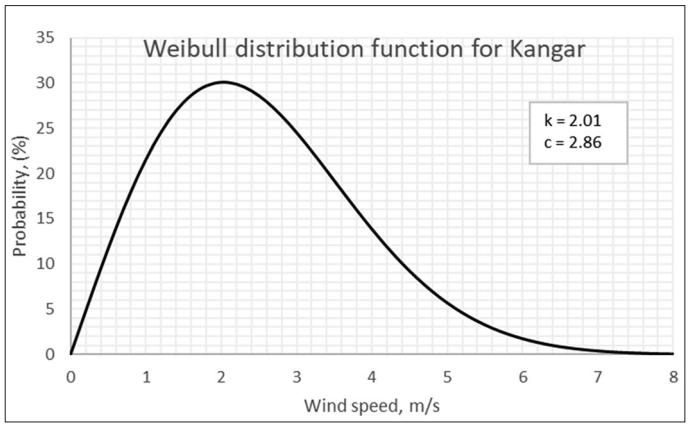

Figure 9: **(a)** Power curve for tip speed ratio (TSR) of 5. (b) Power curve for TSR of 6

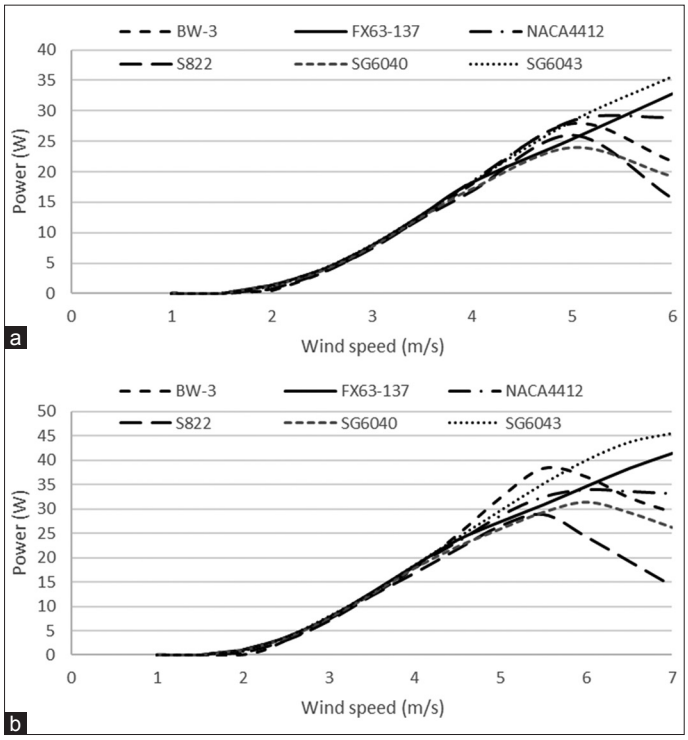

Figure 10: (a) Power coefficient for tip speed ratio (TSR) of 5. (b) Power coefficient for TSR of 6

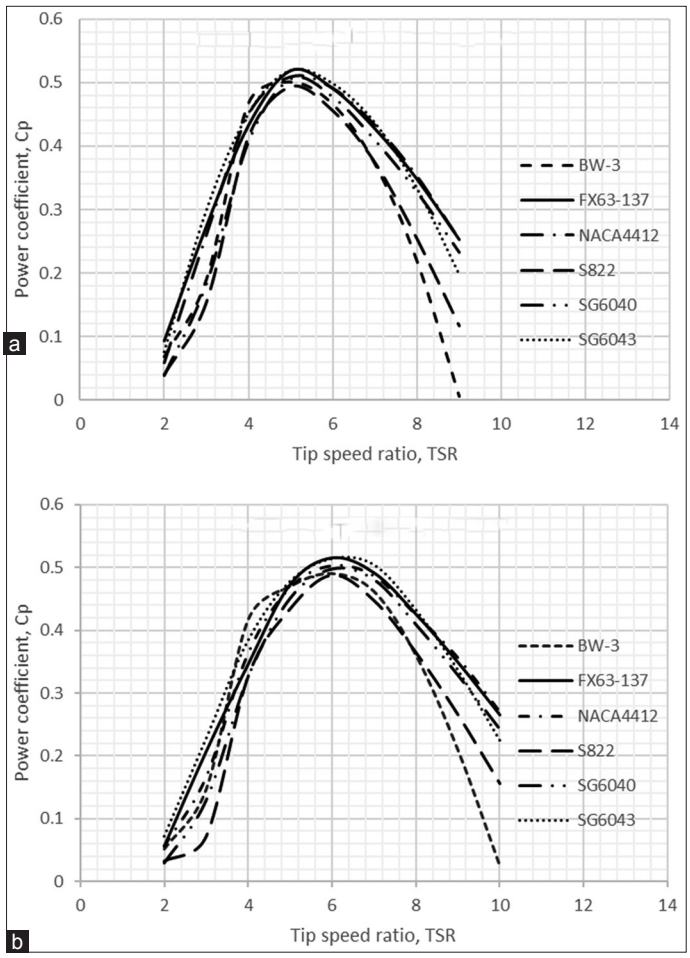

Table 8: Annual energy generation, kWh

Turbines	Annual energy generation, kWh	
	TSR=5	TSR=6
BW-3	59	62
FX63-137	62	63
NACA4412	63	63
S822	55	56
SG6040	56	60
SG6043	64	66

TSR: Tip speed ratio

Table 9: Maximum power coefficient at TSR of 5 and 6

Turbine	Maximum power coefficient, $C_{P, Max}$	
	TSR=5	TSR=6
BW-3	0.5003	0.4910
FX63-137	0.5190	0.5148
NACA4412	0.5086	0.5022
S822	0.4945	0.4878
SG6040	0.5059	0.4986
SG6043	0.5194	0.5141

Table 10: Cut-in speed of design CS-SHAWTs

Turbines	Cut-in speed, m/s	
	TSR=5	TSR=6
BW-3	1.50	2.08
FX63-137	1.50	1.76
NACA4412	1.65	1.75
S822	1.82	1.58
SG6040	1.64	1.78
SG6043	1.78	1.88

5.3. Capacity Factor

The expression of AEG and the power coefficient of the six turbines have been presented. Nonetheless, it is inadequate to know the machine's performance merely based on these two expressions. Therefore, the capacity factor is introduced to compare the six turbines' performance, which is to determine how much electricity of the designed CS-SHAWTs produces when it is operating at its maximum capacity throughout a one-year period. The AEG and the rated power are the two important parameters determining the capacity factor of the machine and the equation is presented as follows:

$$\text{Capacity Factor, } CF = \frac{E_{generated}}{P_{Rated} \times 8760} \quad (16)$$

Table 11 depicts the capacity factor of the designed CS-SHAWTs at TSR of 5 and 6. All the turbines achieved above 50% of capacity factor, which indicates that the designed CS-SHAWTs have high potential for low wind regimes installation in Malaysia. For TSR of 5, NACA4412 turbine has the highest capacity factor of 56.7% and the lowest is SG6040 turbine with only 50.7%. For TSR of 6, SG6043 turbine outperformed other turbines with 58.8%, while S822 turbine has the least capacity factor of 52.5%. The main factor that affects capacity factor is the type of airfoil of the blade. Choice of airfoil will directly influence the characteristics of wind turbines such as cut-in speed, cut-out speed, and rated power, etc.

Table 11: Capacity factor (%)

Turbines	Capacity factor, (%)	
	TSR=5	TSR=6
BW-3	54.0	57.8
FX63-137	54.7	56.0
NACA4412	56.7	57.4
S822	50.9	52.5
SG6040	50.7	55.0
SG6043	56.4	58.8

TSR: Tip speed ratio

Typically, the commercially available wind turbines' capacity factors lie in between 20 to 35% only (Bhadra et al., 2005; Nicolas 2009). It is worthy to note that capacity factor is not equivalent to efficiency of the turbine. Efficiency is the account for energy losses of how much of the captured wind is converted into useful energy, after going through the conversion process.

6. CONCLUSION AND RECOMMENDATION

This paper aimed at the performance analysis of optimizing rotor blade design for constant speed – small horizontal axis wind turbine (CS-SHAWT) based on six low Reynolds number airfoils. The performance analysis is performed by blade element momentum theory. The results of CS-SHAWTs at TSR of 5 and 6 for different airfoils are investigated. The selected airfoils have their strengths in different aspects.

The results obtained for the maximum power coefficient at the design wind speed of 3.5 m/s can achieve above 50% for a 3-bladed, 1.1m rotor diameter CS-SHAWT. The BW-3 and FX63-137 airfoils have an impressive low cut-in speed at 1.50 m/s for TSR of 5. Lower TSR is desirable for low wind sites, and as per this study, TSR of 5 is preferable compared to TSR of 6. In the aspects of annual energy generated, CS-SHAWTs can reach 60 kWh and above. Though the generated value may be insufficient to fulfil the per capita demand; however, this designed CS-SHAWT has a high potential to be clustered as a wind farm in Malaysia due to its high capacity factor which is reachable up to 55%.

To enhance either in the aspects of cut-in speed or annual energy generated of the designed CS-SHAWT, the installation of the vortex generator method can help in improving airflow near the surface of blade by increasing the blade aerodynamic.

REFERENCES

Azad, A.K., Saha, M. (2012), Wind power: A renewable alternative source of green energy. International Journal of Basic and Applied Science, 1, 193-199.

Bergey Wind Power Co. USA. (2018), Available from: http://www.bergey.com/contact_bergey.

Bhadra, S., Kastha, D., Banerjee, S. (2005), Wind Electrical Systems. Oxford: Oxford University Press.

Burton, T., Tiwari, K. (2001), Wind Energy Handbook. Hoboken: John Wiley and Sons, Ltd.

Clausen, P.D., Wood, D.H. (1999), Research and development issues for small wind turbines. Renewable Energy, 16, 922-927.

Duləu, L.I., Abrudean, M., Bică, D. (2014), Effects of Distributed Generation on Electric Power Systems. The 7th International Conference Interdisciplinarity in Engineering (INTER-ENG 2013), Procedia Technology, 12, 681-686.

Fasel, H.F., Grossm, A. (2011), Numerical Investigation of Different Wind Turbine Airfoils. Tucson, Orlando, Florida: The University of Arizona.

Giguere, P., Selig, M.S. (1997), Low Reynolds number Airfoils for small horizontal axis wind turbines. Wind Engineering, 21, 379.

Giguere, P., Selig, M.S. (1998), New airfoils for small horizontal axis wind turbines. ASME Journal of Solar Energy Engineering, 120, 108-114.

Gipe, P. (2004), Wind Power: Renewable Energy for Home, Farm, and Business. White River Junction: Chelsea Green Publishing Company.

IRENA. (2017), Renewable Energy Prospects for India, a Working Paper Based on RE Map. Abu Dhabi: The International Renewable Energy Agency (IRENA-2017). Available from: http://www.irena.org/remap.

Irwanto, M. Gomesh, N., Mamat, M.R., Yusoff, Y.M. (2014), Assessment of wind power generation potential in Perlis, Malaysia. Renewable and Sustainable Energy Reviews, 38, 296-308.

Manoj, K.C., Roy, A. (2015), Design and optimization of a small wind turbine blade for operation at low wind speed. World Journal of Engineering, 12(1), 83-94.

Manwell, J., Jon, G. (2009), Wind Energy Explained: Theory, Design and Application. United States: John Wiley and Sons Ltd.

McGranahan, B.D., Selig, M.S. (2004), Aerodynamic Tests of Six Airfoils for use on Small Wind Turbines. Illinois: University of Illinois at Urbana-Champaign Urbana.

MMD. (2016), Malaysian Meteorological Department Wind Energy Data; 2016. Available from: http://www.met.gov.my/penerbitan/laporantahunan.

Munish, M. (2018), Optimization of distributed generation based hybrid renewable energy system for a DC micro-grid using particle swarm optimization. Distributed Generation and Alternative Energy Journal, 33(4), 7-25.

Nicolas, B. (2009), Capacity factor of wind power realized values vs. estimates. Energy Policy, 37, 2679-2688.

NREL., Airfoils, Inc. (2014), Available from: https://www.wind.nrel.gov/airfoils/Shapes/S822_Shape.html.

Ozgener, O., Ozgener, L. (2007), Exergy and reliability analysis of wind turbine systems: A case study. Renewable and Sustainable Energy Reviews, 11, 1811-1826.

Palanichamy, C. (2015), Exploring Wind Energy as a Potential Energy Source. Borneo: Borneo Post Online.

Palanichamy, C., Nasir, M., Veeramani, S. (2015), Wind cannot be Directed but Sails can be Adjusted for Malaysian Renewable Energy Progress. IOP Conference Series, No. 12028. Materials Science and Engineering. p78.

Ronit, K.S., Radiuddin, A.M. (2013), Blade design and performance testing of a small wind turbine rotor for low wind speed applications. Renewable Energy, 50, 812-819.

Samuel, O.A., Polinder, H., Ferreira, J.A. (2013), Comparison of energy yield of small wind turbines in low wind speed areas. IEEE Transactions on Sustainable Energy, 4(1), 42-49.

Tan, W.W., Palanichamy, C. (2018), Commercial Wind Turbines' Suitability for Low-Wind Areas in Malaysia. Pacifico Yokohama, Yokohama, Japan: International Conference.

EWEA. (2018), European Wind Energy Association. The European offshore wind industry - key trends and statistics 2017. Available from: https://windeurope.org/about-wind/statistics/offshore/european-offshore-wind-industry-key-trends-statistics-2017. [Last accessed on 2018 Nov 19]

Wortmann. (2018), FX63-137 AIRFOIL. Available from: http://www.airfoildb.com/airfoils/1120.

Yong, K.H., Ibrahima, M.Z., Ismaila, A. (2011), Wind Mapping in Malaysia Using Inverse Distance Weighted Method. Empowering Science and Technology Innovation towards a Better Tomorrow, 35, 60-67.